JOURNAL OF COMPUTATIONAL PHYSICS 56, 15–27 (1984)

Analytical Prediction of Two-Dimensional Potential Flow Due to Fixed Vortices in a Rectangular Domain

YOUNGKI CHOI* AND JOSEPH A. C. HUMPHREY†

Department of Mechanical Engineering, University of California, Berkeley, California 94720

Received August 9, 1983; revised January 13, 1984

An analytical method is presented which solves 2-D potential flow in a rectangular domain containing multiple vortices fixed in space. A double infinite image system is used to satisfy the zero normal velocity boundary condition. Because of its accuracy and speed of calculation, the solution can serve as the building block for predicting wall-driven cavity flows at high Reynolds number using the random vortex method of Chorin. This communication outlines the derivation of the analytical method and presents tests performed to check its validity. Two limiting flow cases predicted from the analysis correspond respectively to: (a) the line vortex problem between parallel planes; and (b) the vortex pair problem in an infinite domain. The results obtained show excellent agreement with established exact solutions.

1. INTRODUCTION

The closed cavity problem with one sliding wall driving a fluid within it has been used frequently as a test for finite difference and finite element methods [1–8] in fluid mechanics. However, it has been difficult and expensive to obtain accurate results for high Reynolds number flow due to the large computer time and storage requirements for detailed calculations. Finite difference and finite element techniques require fairly refined grids in regions of sharp velocity gradients such as recirculation zones and near walls in order to reduce numerical diffusion errors. Shestakov [9] solved the wall-driven cavity flow problem by combining a finite difference method with the random vortex blob method of Chorin [10]. The latter is a grid-free method, with an error which is proportional to the inverse square root of the Reynolds number. Initial difficulties experienced with rates of convergence of the vortex blob method near boundaries were overcome by Chorin [11] through the development of the random vortex sheet method. Our long-term objective is to solve the wall-driven closed cavity flow problem at high Reynolds number using the random vortex blob method in the bulk of the flow and the random vortex sheet method near boundaries. Of special interest is the case of a non-isothermal flow with buoyant effects. As a first step

* Research graduate student.
† Associate Professor.

0021-9991/84 $3.00

581/56/1-2

towards this objective, we have focused on the problem of predicting 2-D potential flow inside a rectangle containing one or several vortices fixed in space. This solution can then be used to generate the required vortex sheets at solid walls and to obtain the velocity of a vortex blob due to surrounding vortex blobs.

Ghoniem [12] has solved turbulent flow over a backward facing step using the random vortex method. In this 2-D problem, the Schwarz–Christoffel conformal mapping method is used to derive the potential flow. However, in a closed cavity it is difficult to use conformal mapping because the vortex blobs distribute to infinity in the transformed plane

Greenhill [13] solved for the path of a vortex in a rectangular domain due to its own images; he analyzed several rectangular configurations but attention was confined to the path of a single vortex. He also solved for the stream function due to a vortex located at the center of a rectangular domain using symmetry conditions. This solution is of special interest to the present study for validation purposes.

This communication presents the analytical solution for potential flow in a rectangular domain due to one or several vortices fixed at arbitrary locations within it. The solution provides the stream function and the velocity components in closed form using elliptic functions. The analysis presents an advancement over the work of Greenhill since it allows calculations to be performed in closed form at arbitrary positions within rectangular domains.

2. Analysis

Let us fix a single real vortex at position (x_1, y_1) inside a 2-D rectangular domain of dimensions $a = 3$, $b = 2$ as shown in Fig. 1. The stream function satisfies

$$\nabla^2 \psi = -\xi \tag{1}$$

where

$$u = \frac{\partial \psi}{\partial y}, \qquad v = -\frac{\partial \psi}{\partial x}. \tag{2}$$

The vorticity is then described in terms of

$$\xi = \Gamma \delta(x - x_1, y - y_1) \tag{3}$$

where δ is the Dirac δ-function and Γ is the vortex strength defined by

$$\Gamma = \lim_{\Delta A \to 0} \int_{\Delta A} \xi \, dA \tag{4}$$

where ξ is acting on area ΔA. The general solution of Eqs. (1) and (3) is

$$\psi = -\Gamma \ln \sqrt{(x - x_1)^2 + (y - y_1)^2}. \tag{5}$$

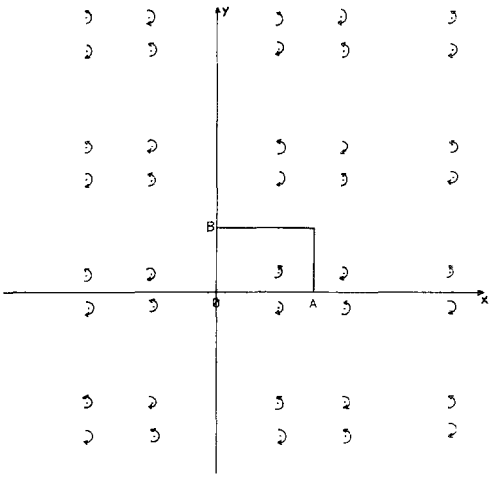

FIG. 1. The rectangular configuration and double infinite image system.

The double infinite image system shown in Fig. 1 is used to satisfy the impermeable normal boundary condition, $\mathbf{v} \cdot \mathbf{n} = 0$. The coordinates of the images are given by

$$(x_1 + 2ma,\ y_1 + 2nb), \qquad (2a - x_1 + 2ma,\ 2b - y_1 + 2nb)$$

in the positive direction and

$$(2a - x_1 + 2ma,\ y_1 + 2nb), \qquad (x_1 + 2ma,\ 2b - y_1 + 2nb)$$

in the negative direction, where m and n are integers and counter-clockwise vortices are taken as positive. Using Eq. (5) for each image and summing over all images yields the stream function at an arbitrary position (x, y). The result is

$$\begin{aligned}
\psi = &-\Gamma \ln \prod_{n=-\infty}^{n=\infty} \prod_{m=-\infty}^{m=\infty} \sqrt{(x - x_1 - 2ma)^2 + (y - y_1 - 2nb)^2} \\
&-\Gamma \ln \prod_{n=-\infty}^{n=\infty} \prod_{m=-\infty}^{m=\infty} \sqrt{(x - 2a + x_1 - 2ma)^2 + (y - 2b + y_1 - 2nb)^2} \\
&+\Gamma \ln \prod_{n=-\infty}^{n=\infty} \prod_{m=-\infty}^{m=\infty} \sqrt{(x - x_1 - 2ma)^2 + (y - 2b + y_1 - 2nb)^2} \\
&+\Gamma \ln \prod_{n=-\infty}^{n=\infty} \prod_{m=-\infty}^{m=\infty} \sqrt{(x - 2a + x_1 - 2ma)^2 + (y - y_1 - 2nb)^2}.
\end{aligned} \tag{6}$$

Note that this can be written as

$$\begin{aligned}
\psi = &F(x - x_1, y - y_1) + F(x - 2a + x_1, y - 2b + y_1) \\
&- F(x - x_1, y - 2b + y_1) - F(x - 2a + x_1, y - y_1)
\end{aligned} \tag{7}$$

where

$$F(x,y) = -\frac{\Gamma}{2} \ln \prod_{n=\infty}^{n=-\infty} \prod_{m=\infty}^{m=-\infty} [(x+2ma)^2 + (y+2nb)^2]. \tag{8}$$

Using the relationship $a^2 + b^2 = (a+bi)(a-bi)$, where $i = \sqrt{-1}$, we can write the last expression as

$$\begin{aligned} F(x,y) = &-\frac{\Gamma}{2} \ln \left[(x+yi) \prod_{n\neq 0} \prod_{m\neq 0} \left(1 + \frac{x+yi}{2ma+2nbi}\right) \right] + G(m,n) \\ &-\frac{\Gamma}{2} \ln \left[(x-yi) \prod_{n\neq 0} \prod_{m\neq 0} \left(1 + \frac{x-yi}{2ma+2nbi}\right) \right] \end{aligned} \tag{9}$$

where

$$G(m,n) = -\frac{\Gamma}{2} \ln \prod_{n\neq 0} \prod_{m\neq 0} (2ma+2nbi)^2. \tag{10}$$

It is possible to express this result in terms of the elliptic functions $sn(u,k)$, $cn(u,k)$ and $dn(u,k)$ to obtain an expression that can be easily calculated using the Landen transformation. The resulting expression for the stream function is (see Appendix A)

$$\begin{aligned} \psi = &P(x-x_1, y-y_1) + P(x-2a+x_1, y-2b+y_1) \\ &- P(x-x_1, y-2b+y_1) - P(x-2a+x_1, y-y_1) \end{aligned} \tag{11}$$

where

$$P(x,y) = -\frac{\Gamma}{2} \ln \left[1 - cn^2\left(\frac{Kx}{a}, k\right) cn^2\left(\frac{Ky}{a}, k'\right) \right] \tag{12}$$

and

$$K = \int_0^{\pi/2} \frac{d\phi}{\sqrt{1-k^2 \sin^2\phi}}, \qquad K' = \int_0^{\pi/2} \frac{d\phi}{\sqrt{1-k'^2 \sin^2\phi}}. \tag{13}$$

Note that k is the modulus, $k' = \sqrt{1-k^2}$ and $K/K' = a/b$. Finally,

$$\begin{aligned} u = &P_y(x-x_1, y-y_1) + P_y(x-2a+x_1, y-2b+y_1) \\ &- P_y(x-x_1, y-2b+y_1) - P_y(x-2a+x_1, y-y_1) \end{aligned} \tag{14}$$

$$\begin{aligned} v = &-P_x(x-x_1, y-y_1) - P_x(x-2a+x_1, y-2b+y_1) \\ &+ P_x(x-x_1, y-y_1) + P_x(x-2a+x_1, y-y_1) \end{aligned} \tag{15}$$

where

$$P_y = -\frac{K\Gamma}{a} \frac{cn^2(Kx/a, k)\, cn(Ky/a, k')\, sn(Ky/a, k')\, dn(Ky/a, k')}{[1 - cn^2(Kx/a, k)\, cn^2(Ky/a, k')]} \tag{16}$$

$$P_x = -\frac{K\Gamma}{a} \frac{cn^2(Ky/a, k')\, cn(Kx/a, k)\, sn(Kx/a, k)\, dn(Kx/a, k)}{[1 - cn^2(Kx/a, k)\, cn^2(Ky/a, k')]}. \tag{17}$$

Since the equation of motion and the impermeable and slip boundary conditions are linear, superposition can be used to apply this method to the case of potential flow in a rectangle containing multiple spatially fixed vortices.

3. Testing

3.1. *Comparison of Present Analysis with Established Exact Solutions*

The solution for the case of a single vortex contained in a rectangular domain with $b/a \to \infty$ is derived and compared with the solution of the line vortex problem between parallel planes. Let the single vortex ξ_1 be fixed at (x_1, y_1) and take the aspect ratio (b/a) as infinite. For this case, k, k', K and K' become

$$\frac{a}{b} = \frac{K}{K'} = 0; \quad k = 0; \quad k' = 1; \quad K = \pi/2; \quad K' = \infty. \tag{18}$$

Displacing the origin of the coordinate system to the center of the rectangular domain allows use of the relations

$$\begin{aligned} cn(x, 0) &= \cos x \\ cn(x, 1) &= \operatorname{sech} x. \end{aligned} \tag{19}$$

The simplified expression for Eq. (11) is

$$\psi = -\frac{\Gamma}{2} \ln \frac{(\cosh(\pi(y - y_1)/a) - \cos(\pi(x - x_1)/a))}{(\cosh(\pi(y - y_1)/a) - \cos(\pi(x - a + x_1)/a)}. \tag{20}$$

This analytical result corresponds exactly to the solution of the line vortex problem between parallel planes derived in Appendix B.

A second test case was performed, essentially corresponding to a pair of counter-rotating vortices in an infinite domain. This problem was approximated by positioning the real vortices ξ_1, ξ_2 at the locations (0, 1) and (0, −1) in a square of sides $a = b = 3000$ (i.e., very large). The vortex strengths Γ_1 and Γ_2 were fixed to be equal and opposte in sign. The velocity components u and v at $y = 0$ were obtained by superposition of the analytical solution given by Eqs. (14) and (15) for each vortex.

The well-known solution [17] of the vortex pair problem in this case is

$$u = \frac{2x^2 - 2(y^2 - 1)}{[x^2 + (y-1)^2][x^2 + (y+1)^2]}$$
$$v = \frac{4xy}{[x^2 + (y-1)^2][x^2 + (y+1)^2]}. \tag{21}$$

A comparison between present calculations and the exact solution of the vortex pair problem is given in Fig. 2 and shows excellent agreement.

Finally, a comparison was made between the present analysis and Greenhill's [13] solution for the stream function due to a single vortex located at the center of a rectangular domain. Displacing the origin of the coordinate system to the center of the rectangular domain and fixing the vortex at (0, 0), after some algebraic manipulation, allows Eq. (11) to be rewritten as

$$\psi = -\frac{\Gamma}{2} \ln \frac{[1 - cn(2Kx/a, k)\, cn(2Ky/a, k')]}{[1 + cn(2Kx/a, k)\, cn(2Ky/a, k')]}. \tag{22}$$

This analytical result corresponds exactly to Greenhill's [13] solution.

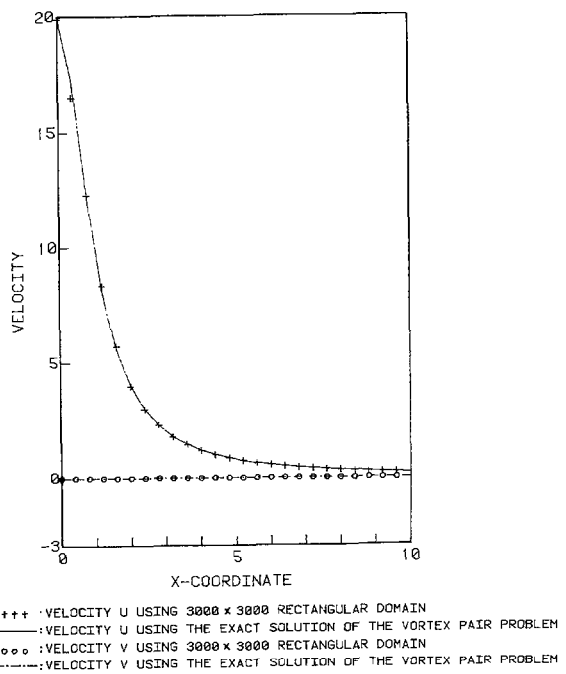

FIG. 2. Comparison between the limiting case solution of the infinite rectangular domain and the exact solution of the vortex pair problem. Vortex position $\xi_1(0, 1)$, $\xi_2(0, -1)$, strength $\Gamma_1 = -10$, $\Gamma_2 = 10$.

The above comparisons between established exact solutions and results derived from the present analysis establish confidence in the latter.

3.2. *Potential Flow in a Rectangle Containing One or More Fixed Vortices*

Let 4 real vortices ξ_1, ξ_2, ξ_3, ξ_4 be fixed in a rectangular domain $a = 3$, $b = 2$ at the arbitrary locations (1, 0.5), (0.5, 1.5), (2.3, 1.7), (1.8, 0.8). The configuration of interest is shown in Fig. 3. Velocity profiles along the plane $y = 1$ were calculated using Eqs. (14) and (15). To check present results, approximate solutions for this case were obtained from the truncated series solutions using $50 * 50 * 4$ images and $5 * 5 * 4$ images around the rectangle. The comparison is shown in Fig. 4. The maximum percentage error relative to the analytical result was found to be 3.8 % for 100 images and 0.1 % for 10,000 images. The approximate truncated series solution converges to the analytical result with an increase in the number of images used.

It is possible to calculate the velocity of a vortex due to its own images and the influence of other vortices by combining the present analytical solution with Greenhill's solution [13]. This is desirable because the result is needed, together with the wall velocity, to solve the wall-driven closed cavity flow problem using the random vortex method. First, the velocity of a vortex due to its own images is found using Greenhill's solution [13]. Greenhill showed that the stream function at vortex position (x_1, y_1) due to its own images is given by

$$\psi = -\frac{\Gamma}{2} \ln \left[1 + cs^2 \left(\frac{2Kx_1}{a}, k \right) + cs^2 \left(\frac{2Ky_1}{a}, k' \right) \right]. \tag{23}$$

From this stream function, the velocity components u and v can be found:

$$u = \frac{K\Gamma cn(2Ky_1/a, k')\, dn(2Ky_1/a, k')}{a[1 + cs^2(2Kx_1/a, k) + cs^2(2Ky_1/a, k')]\, sn^3(2Ky_1/a, k')} \tag{24}$$

$$v = \frac{-K\Gamma cn(2Kx_1/a, k)\, dn(2Kx_1/a, k)}{a[1 + cs^2(2Kx_1/a, k) + cs^2(2Ky_1/a, k')]\, sn^3(2Kx_1/a, k)}. \tag{25}$$

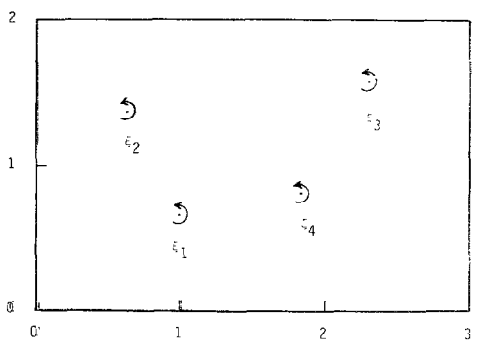

FIG. 3. Configuration examined for the case of multiple vortices.

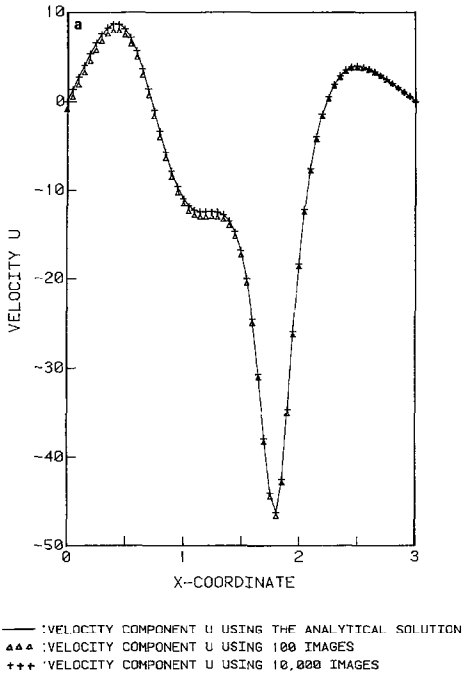

FIG. 4a. Comparison between the analytical solution and the approximate results at $Y = 1$ in a rectangle $A = 3$, $B = 2$. Vortex position $\xi_1(1, 0.5)$, $\xi_2(0.5, 1.5)$, $\xi_3(2.3, 1.7)$, $\xi_4(1.8, 0.8)$. Vortex strength $\Gamma_1 = 10$, $\Gamma_2 = 10$, $\Gamma_3 = 10$, $\Gamma_4 = 10$.

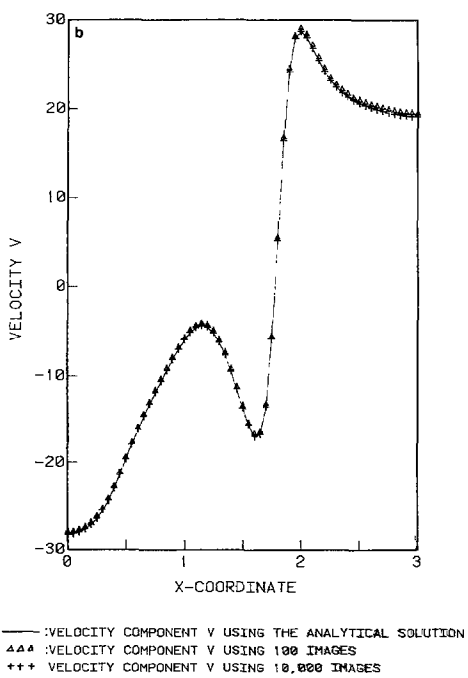

FIG. 4b. Comparison between the analytical solution and the approximate results at $Y = 1$ in a rectangle $A = 3$, $B = 2$. Vortex position $\xi_1(1, 0.5)$, $\xi_2(0.5, 1.5)$, $\xi_2(2.3, 1.7)$, $\xi_4(1.8, 0.8)$. Vortex strength $\Gamma_1 = 10$, $\Gamma_2 = 10$, $\Gamma_3 = 10$, $\Gamma_4 = 10$.

TABLE I

The Differences between Calculations of Velocity Using the Analytical Solution and the Approximate Image Method at the Vortex Position (1.0, 0.5) in a Rectangular Domain with $a = 3$, $b = 2$. Four Vortices ξ_i at (1.0, 0.5), (0.5, 1.5), (2.3, 1.7), (1.8, 0.8) with $\Gamma_i = 10$

X-Direction Velocity U

Position				
x	y	U_a	U_n	$[(U_a - U_n)/U_a]$ 100
1.0	0.5	18.7854652	18.7821579	0.0176059
0.5	1.5	−11.7206106	−11.7247639	−0.0354355
2.3	1.7	−24.6013451	−24.6025257	−0.0047991
1.8	0.8	6.3184361	6.3164458	0.0315002

Y-Direction Velocity V

Position				
x	y	V_a	V_n	$[(V_a - V_n)/V_a]$ 100
1.0	0.5	−7.8478298	−7.8453555	0.0315286
0.5	1.5	−11.8070669	−11.8062372	0.0070271
2.3	1.7	5.7389870	5.7394867	−0.0087076
1.8	0.8	7.6620049	7.6640153	−0.0262379

Note. U_a, V_a: Velocity components of vortex due to its own images and the surrounding vortices using the analytical solution. U_n, V_n: Velocity components of vortex due to its own images and the surrounding vortices using 6400 images.

Using these relations, the velocity components at, for example, (1, 0.5) due to the images of ξ_1 at this location can be found. These components are then added to the velocity components at the same point, due to the surrounding vortices and their images, using the analytical solution. The velocity components of the other vortices are obtained analogously. Table I provides a comparison between the above analytical procedure and approximate results using $20 * 20 * 4 * 4$ images. The test shows that a combination of the analytical solution with Greenhill's solution corresponds closely to the approximate solution using images.

4. Conclusions

An analytical solution for 2-D potential flow inside a rectangle with multiple vortices has been derived and tested. This closed form solution gives the stream function and velocity components at arbitrary positions due to vortices and their infinite images in terms of elliptic functions. The main advantage of the analytic

solution is that it requires only 6 iterations for convergence, while corresponding numerical evaluations using over 10^4 images to attain the same degree of accuracy require over 10^4 iterations. In calculations using the random vortex method, if n vortex blobs are present in the fluid, then $O(n^2)$ interactions must be computed per time step. If truncated series (approximate) numerical calculation procedures are used, computing times will be very long.

The agreement found between the analytical solution and truncated series numerical evaluations suggests that the analytical solution has been correctly derived. In addition, tests with respect to exactly known flow solutions show that the present analysis is physically sound. The analytical results can be used as the building block for calculations of non-isothermal wall-driven cavity flows. This is presently the subject of ongoing research.

APPENDIX A: Proof of Eq. (11) in the Main Text

The Jacobian function H is defined as [14]

$$H(u, k) = \sqrt{\frac{2kk'K}{\pi}}\, u \prod_{n\neq 0} \prod_{m\neq 0} \left[1 + \frac{u}{2mK + 2nK'i}\right] \tag{A-1}$$

where k is the modulus and $K = \int_0^{\pi/2} d\phi/\sqrt{1 - k^2 \sin^2 \phi}$; note also that $k' = \sqrt{1 - k^2}$ and $K' = \int_0^{\pi/2} d\phi/\sqrt{1 - k'^2 \sin^2 \phi}$. Using Eq. (A-1), the first part of $F(x, y)$ given by Eq. (9) in the next is

$$(x + yi) \prod_{n\neq 0} \prod_{m\neq 0} \left(1 + \frac{x + yi}{2ma + 2nbi}\right) = \frac{a}{K} \sqrt{\frac{\pi}{2kk'K}}\, H\left(\frac{Kx}{a} + \frac{Ky}{b}\, i, k\right) \tag{A-2}$$

where $K/K' = a/b$. Similarly:

$$(x - yi) \prod_{n\neq 0} \prod_{m\neq 0} \left(1 + \frac{x - yi}{2ma + 2nbi}\right) = \frac{a}{K} \sqrt{\frac{\pi}{2kk'K}}\, H\left(\frac{Kx}{a} - \frac{Ky}{b}\, i, k\right). \tag{A-3}$$

Combining these results yields

$$F(x, y) = -\frac{\Gamma}{2} \ln \left(\frac{a}{K}\right)^2 \left(\frac{\pi}{2kk'K}\right) H\left(\frac{Kx}{a} + \frac{Ky}{b}\, i, k\right) \times H\left(\frac{Kx}{a} - \frac{Ky}{b}\, i, k\right) + G(m, n). \tag{A-4}$$

The Jacobian functions H and Θ are defined as [15, 16]

$$H(x+yi,k)\,H(x-yi,k)=\frac{\pi}{2k'K}\,[H^2(x,k)\,\Theta^2(yi,k)-H^2(yi,k)\,\Theta^2(x,k)] \tag{A-5}$$

$$H(yi,k)=i\sqrt{\frac{k}{k'}}\exp\left(\frac{\pi y^2}{4KK'}\right)H(y,k')\,\frac{\Theta(0,k)}{\Theta(0,k')} \tag{A-6}$$

$$\Theta(yi,k)=\sqrt{\frac{k}{k'}}\exp\left(\frac{\pi y^2}{4KK'}\right)H(y+K',k')\,\frac{\Theta(0,k)}{\Theta(0,k')} \tag{A-7}$$

$$\Theta(0,k)=\sqrt{\frac{2k'K}{\pi}},\qquad \Theta(0,k')=\sqrt{\frac{2kK'}{\pi}}. \tag{A-8}$$

From Eqs. (A-4) to (A-8) it follows that

$$\begin{aligned}F(x,y)&=-\frac{\Gamma}{2}\ln\left(\frac{a^2\pi^2}{4K^3K'kk'^2}\right)\exp\left(\frac{\pi Ky^2}{2K'a^2}\right)\\&\quad\times\left[H^2\left(\frac{Kx}{a},k\right)H^2\left(\frac{Ky}{a}+K',k'\right)+H^2\left(\frac{Ky}{a},k'\right)\Theta^2\left(\frac{Kx}{a},k\right)\right]\\&\quad+G(m,n)\\&=-\frac{\Gamma}{2}\ln\left(\frac{\pi^2ab}{4K^3K'kk'^2}\right)\left[\frac{H^2(Kx/a,k)\,H^2(Ky/a+K',k')}{\Theta^2(Kx/a,k)\,\Theta^2(Ky/a,k')}+\frac{H^2(Ky/a,k')}{\Theta^2(Ky/a,k')}\right]\\&\quad\times\Theta^2\left(\frac{Kx}{a},k\right)\Theta^2\left(\frac{Ky}{a},k'\right)-\frac{\Gamma\pi K^2y^2}{K'a^2}+G(m,n).\end{aligned} \tag{A-9}$$

The relations between the elliptic functions $sn(u,k)$, $cn(u,k)$, $dn(u,k)$ and the Jacobian functions H, Θ are [15]

$$\frac{H(u+K,k)}{\Theta(u,k)}=\sqrt{\frac{k'}{k}}\,cn(u,k) \tag{A-10}$$

$$\frac{H(u,k)}{\Theta(u,k)}=\sqrt{k}\,sn(u,k) \tag{A-11}$$

$$sn^2(u,k)+cn^2(u,k)=1. \tag{A-12}$$

Using Eqs. (A-10) to (A-12), Eq. (A-9) becomes

$$\begin{aligned}F(x,y)&=c+P(x,y)-\Gamma\ln\Theta\left(\frac{Kx}{a},k\right)-\Gamma\ln\Theta\left(\frac{Ky}{a},k'\right)\\&\quad-\frac{\Gamma\pi Ky^2}{K'a^2}+G(m,n)\end{aligned} \tag{A-13}$$

where

$$c = -\frac{\Gamma}{2} \ln \frac{\pi^2 ab}{4K'^2 K^2 kk'} \tag{A-14}$$

and

$$P(x, y) = -\frac{\Gamma}{2} \ln \left[1 - cn^2 \left(\frac{Kx}{a}, k \right) cn^2 \left(\frac{Ky}{a}, k' \right) \right]. \tag{A-15}$$

Substituting Eq. (A-13) into Eq. (7) in the text yields

$$\begin{aligned} \psi = {} & P(x - x_1, y - y_1) + P(x - 2a + x_1, y - 2b + y_1) \\ & - P(x - x_1, y - 2b + y_1) - P(x - 2a + x_1, y - y_1). \end{aligned} \tag{A-16}$$

APPENDIX B

The general solution of the line vortex problem between parallel planes is

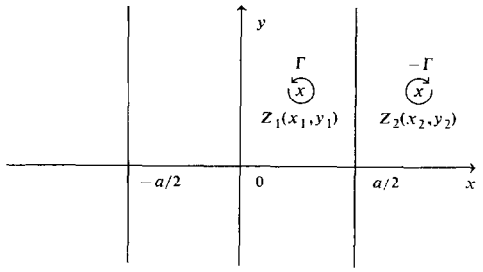

For this case the complex velocity potential Wn becomes

$$\begin{aligned} Wn(Z) &= -i\Gamma \sum_{m=-\infty}^{\infty} \ln(Z - Z_1 + 2ma) + i\Gamma \sum_{m=-\infty}^{\infty} \ln(Z - Z_2 + 2ma) \\ &= -i\Gamma \ln \left[\frac{(\pi(Z - Z_1)/2a) \prod_{m=1}^{\infty} (1 - (Z - Z_1)^2/m^2(2a)^2)}{(\pi(Z - Z_2)/2a) \prod_{m=1}^{\infty} (1 - (Z - Z_2)^2/m^2(2a)^2)} \right]. \end{aligned} \tag{B-1}$$

Using the infinite product form of $\sin x$ [18]:

$$\sin x = x \prod_{m=1}^{\infty} \left(1 - \frac{x^2}{m^2 \pi^2} \right) \tag{B-2}$$

equation (B-2) yields

$$Wn(Z) = -i\Gamma \ln \frac{\sin(\pi(Z - Z_1)/2a)}{\sin(\pi(Z - Z_2)/2a)}. \tag{B-3}$$

For this complex velocity potential the final form of the stream function can be shown to be

$$\psi = -\frac{\Gamma}{2} \ln \frac{[\cosh(\pi(y-y_1)/a) - \cos(\pi(x-x_1)/a)]}{[\cosh(\pi(y-y_1)/a) - \cos(\pi(x-a+x_1)/a)]}. \tag{B-4}$$

This result is identical to Eq. (20) in the text.

ACKNOWLEDGMENTS

The authors are grateful to Dr. A. Ghoniem for helpful discussions relating to this work and to an anonymous reviewer for making valuable suggestions concerning the presentation of our findings. The study was supported by a grant received from the Committee on Research, University of California, Berkeley. Thanks are due to V. Humphrey for the typing of this manuscript.

REFERENCES

1. R. SCHREIBER AND H. B. KELLER, "Efficient Numerical Techniques for Two-Dimensional Steady Flow," Dept. of Comp. Sci., Stanford University, in preparation.
2. K. H. WINTERS AND K. A. CLIFFE, "A Finite Element Study of Laminar Flow in a Square Cavity," UKAERE Harwell Report R-9444, 1979.
3. A. S. BENJAMIN AND V. E. DENNY, *J. Comput. Phys.* **12** (1973), 348–363.
4. M. D. OLSON AND S. Y. TUANN, *in* "Proceedings, 3rd International Conference on Finite Elements in Flow Problems, Banff, Alberta, Canada, 1980," pp. 143–152.
5. M. NALLASAMY AND K. K. PRASAD, *J. Fluid Mech.* **79** (1977), 391–414.
6. R. D. MILLS, *J. Roy. Aero. Soc.* **69** (1965), 714–718.
7. F. PAN AND A. ACRIVOS, *J. Fluid Mech.* **28** (1967), 643–655.
8. J. R. KOSEFF AND R. L. STREET, *J. Fluids Engrg.*, in press.
9. A. SHESTAKOV, "Numerical Solution of Navier–Stokes Equations at High Reynolds Number," Ph.D. thesis, Department of Mathematics, University of California at Berkeley, 1975.
10. A. J. CHORIN, *J. Fluid Mech.* **57** (1973), 785–797.
11. A. J. CHORIN, *J. Comput. Phys.* **27** (1978), 428.
12. A. F. GHONIEM, A. J. CHORIN, AND A. K. OPPENHEIM, *Philos. Trans. Roy. Soc. London Ser. A* **304** (1982), 304–325.
13. A. G. GREENHILL, *Quar. J. Math.* **15** (1878), 24.
14. A. CAYLEY, "An Elementary Treatise on Elliptic Functions," 2nd ed., p. 303, Bell, London, 1895.
15. A. CAYLEY, "An Elementary Treatise on Elliptic Functions." 2nd ed., p. 156, Bell, London, 1895
16. ERSTER BAND, C. G. J. Jacobi's Gesammelte Werke," p. 227, Verlag Von G. Reimer, Berlin, 1881.
17. L. M. MILNE-THOMSON, "Theoretical Hydrodynamics," 5th ed., p. 359, Macmillan, London, 1968.
18. L. M. MILNE-THOMSON, "Theoretical Hydrodynamics." 5th ed., p. 376, Macmillan, London, 1968.